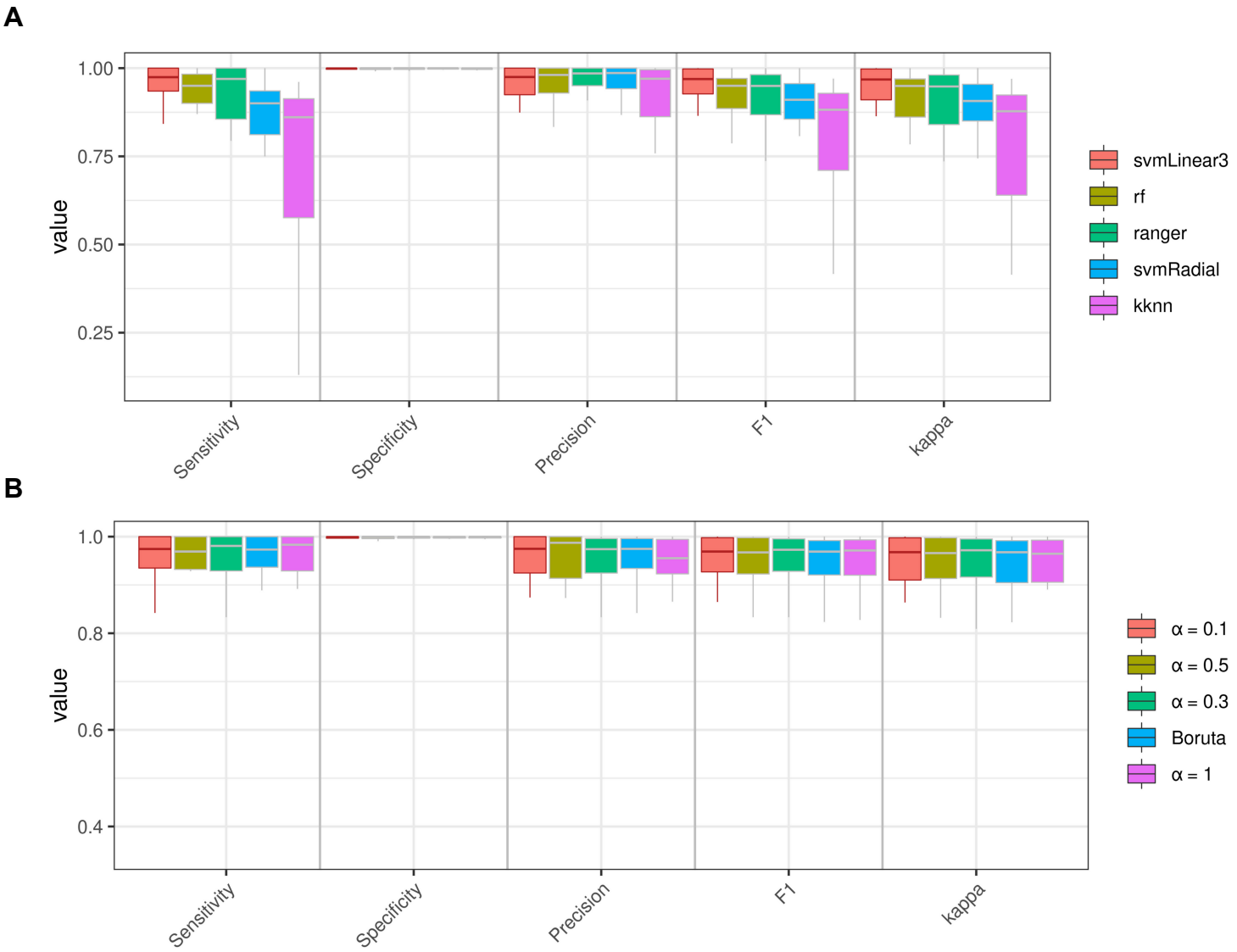

Supplementary Figure S1. Choice of machine learning algorithm contributes to subtype prediction performance. (A) Performance of different machine learning algorithms on the training data (n=1869). Box plots showing classification performance of different machine learning algorithms (svmLinear3, rf, ranger svmRadial and kknn) for averages of individual subtypes. Linear SVM was selected for ALLCatchR because of superior performance on the training data out of five methods tested with an overall accuracy of 0.963 followed by radial SVM (accuracy: 0.957) and KNN (accuracy: 0.901). Overall accuracies are skewed for the impact of large subtypes. Linear SVM was still the best performing method when all subtypes were weighted equally with an average sensitivity of 0.950±0.085 and specificity of 0.998±0.003 **(B)** Features selection methods LASSO and Boruta were applied to account for linear feature to class label interactions as well as non-linear interactions. Different alpha parameters were set in LASSO, where higher values result in a more stringent selection of features. This resulted in different numbers of selected genes for machine training ranging from n=2,802 (union LASSO α=0.1), to n=973 (LASSO α=1). The comparison showed that linear SVM performed stable independent of the feature selection used.

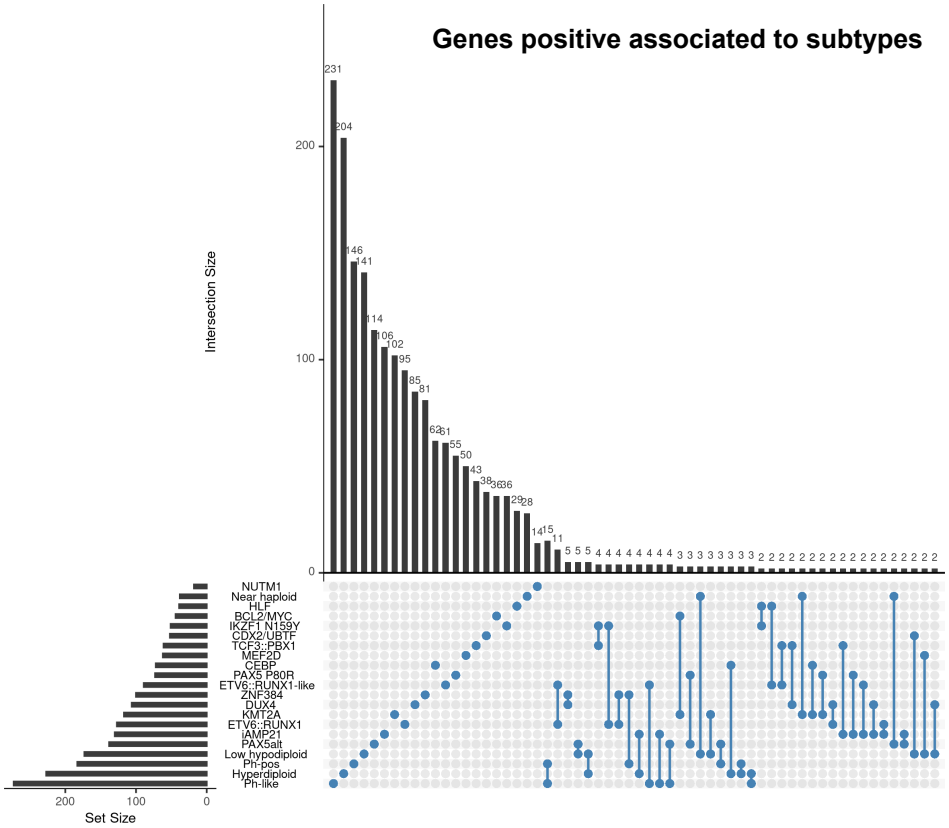

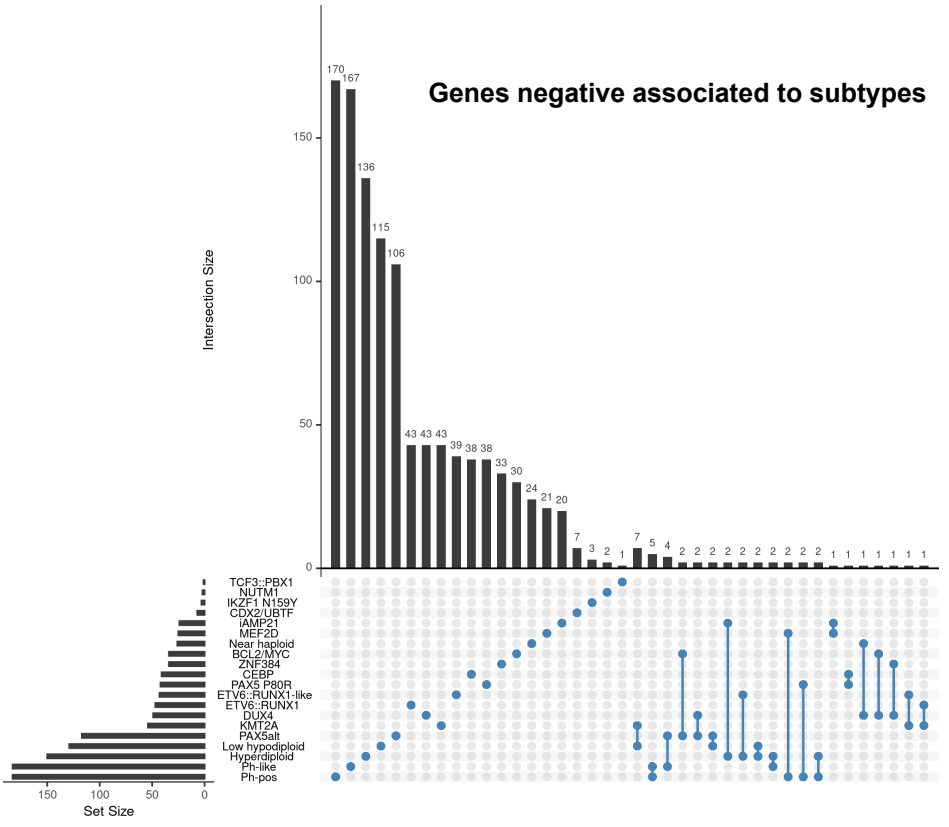

Supplementary Figure S2. The 2,802 LASSO genes used for training ALLCatchR are highly specific for BCP-ALL molecular subtypes. Upset plots showing the number of genes (Set Size) for each subtype and the number of unique and shared genes between subtypes (Intersection Size). In the upper panel, sets with only one gene were excluded.

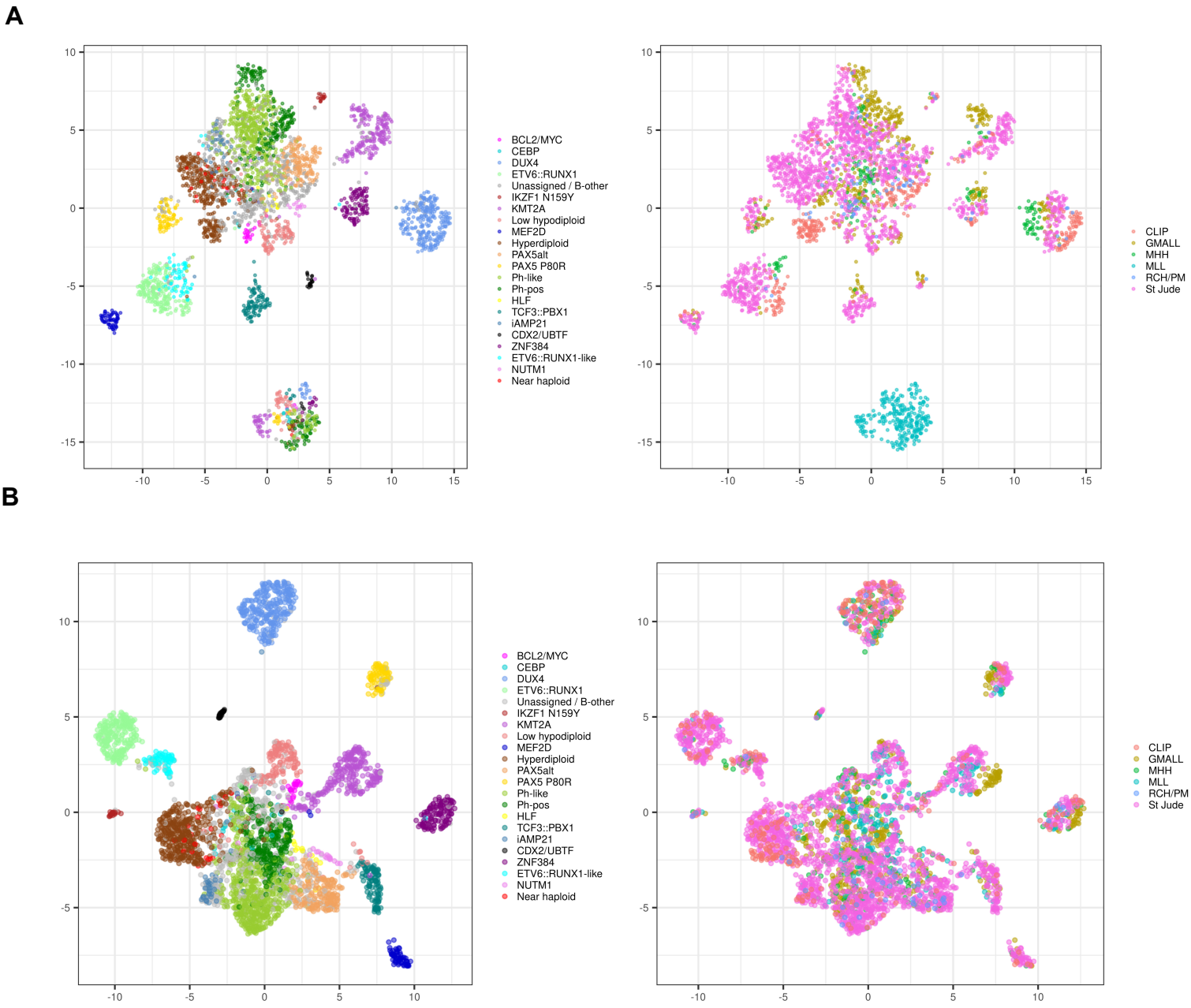

Supplementary Figure S3. Samples separate according to BCP-ALL molecular subtypes based on LASSO genes. (A) UMAP plots depict all samples based on expression of 2,802 LASSO genes (**Supplementary Table S3**) used for training ALLCatchR. Samples group according to their subtypes, but batch effects remain (e.g; MLL cohort). **(B)** Using LASSO gene sets used in (A), single sample gene set analysis was performed with singscore for the n=1,869 training samples, which allowed the computation of a total enrichment score for each sample to each subtype specific gene set. These 21 total enrichment scores for each sample can be used to clearly separate the subtypes as shown here. No more cohort-specific batch effects are observed.

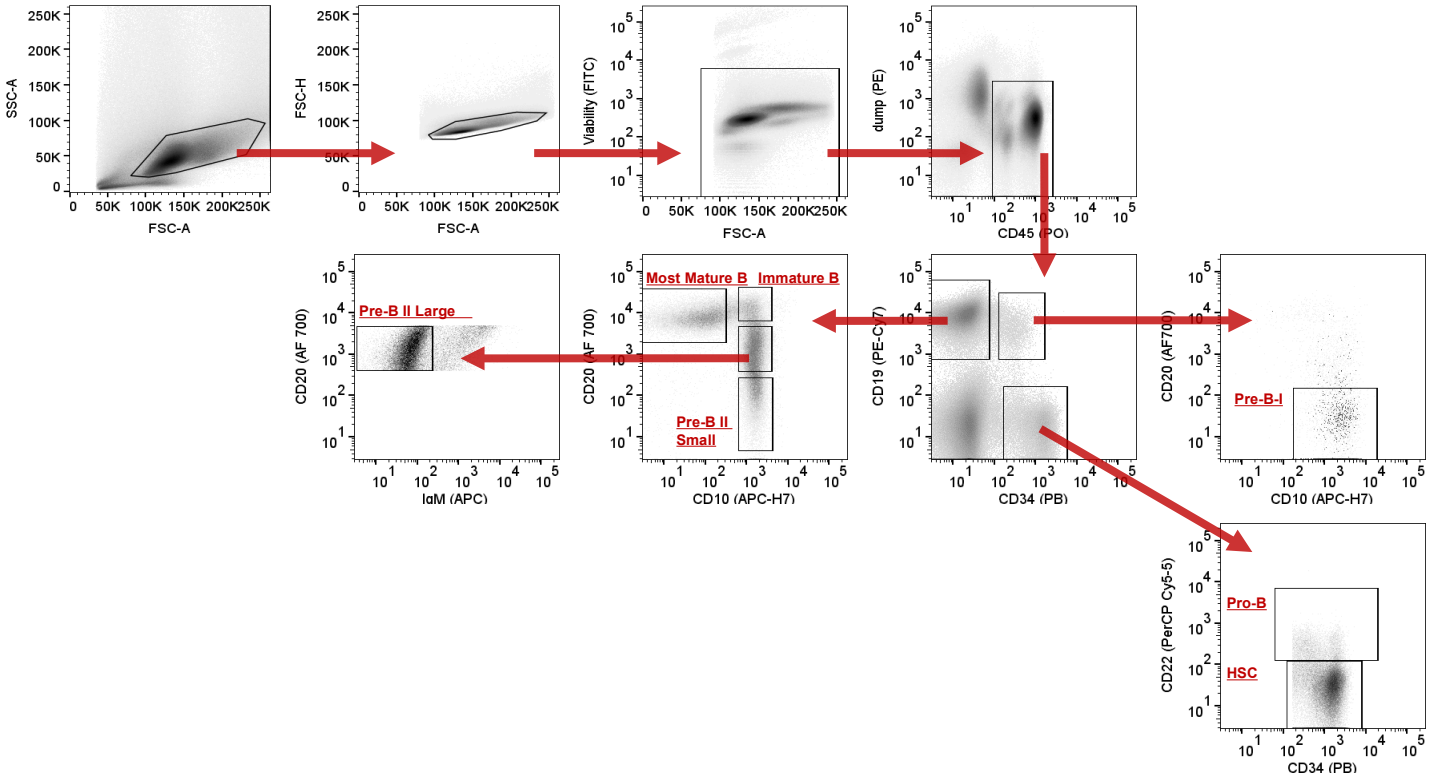

Supplementary Figure S4. Sorting strategy for the isolation of defined B cell precursor subsets. Using a 9-color antibody panel, CD16$^-$ CD36$^-$ CD66b$^-$ CD235a$^-$ CD3$^-$ bone marrow cells were FACS-sorted to seven B lymphoid differentiation stages for downstream analyses. dump: CD3, CD14, CD33, CD56, CD66c, CD138. The antibodies and Fluorochromes used are provied in **Supplementary Table S4**.

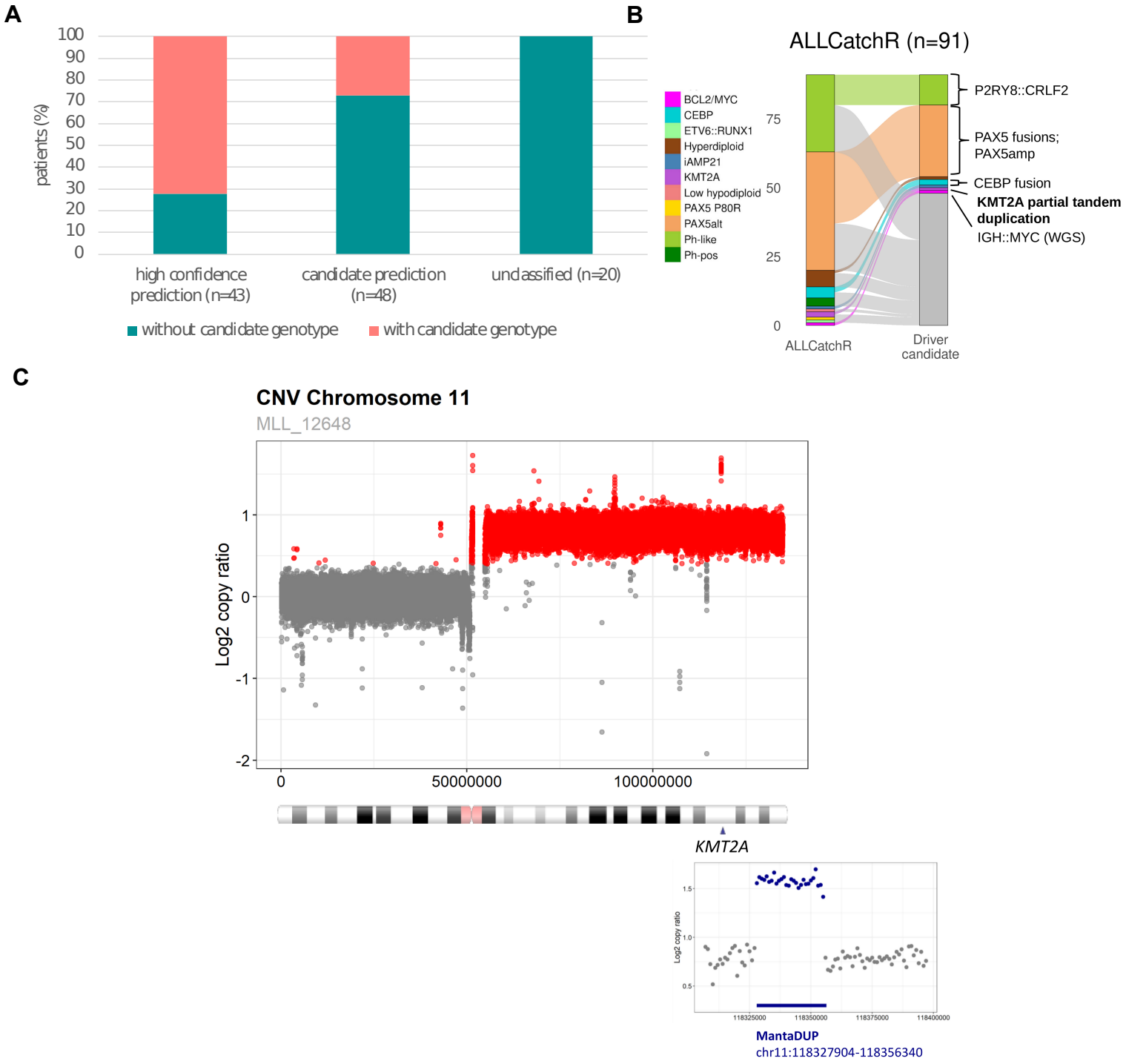

Supplementary Figure S5. Identification of novel candidate subtype assignments in 'unassigned / B-other' samples. (A) A total of n=111 samples of the hold-out-studies were defined 'unassigned / B-other' in the original studies. ALLCatchR provided subtype allocations for n=91 of these samples (**Supplementary Table S5**). The proportions of samples where these predictions could be confirmed by corresponding genomic aberrations are shown. **(B)** Sankey diagrams with detailed representation of ALLCatchR predictions and driver candidates. **(C)** In one sample with a high-confidence KMT2A prediction but absence of KMT2A fusion an i(11)(q10) was identified by whole genome sequencing with additional intrachromosomal tandem duplication at breakpoint chr11:118327904-118356340. This sample showed a pro-B immunophenotype by FACS analysis (positive: cyCD79, CD34, CD38, CD19, CD133, HLA-DR, CD58; weakly positive: CD45, TdT, CD33, CD15, CD65; partially expressed: CD13, CD65; negative: CD117, CD56, CD11b, CD7, CD14, CD2, CD4, MPO, CD3, cyCD22, CD20, CD10).

ALLSorts

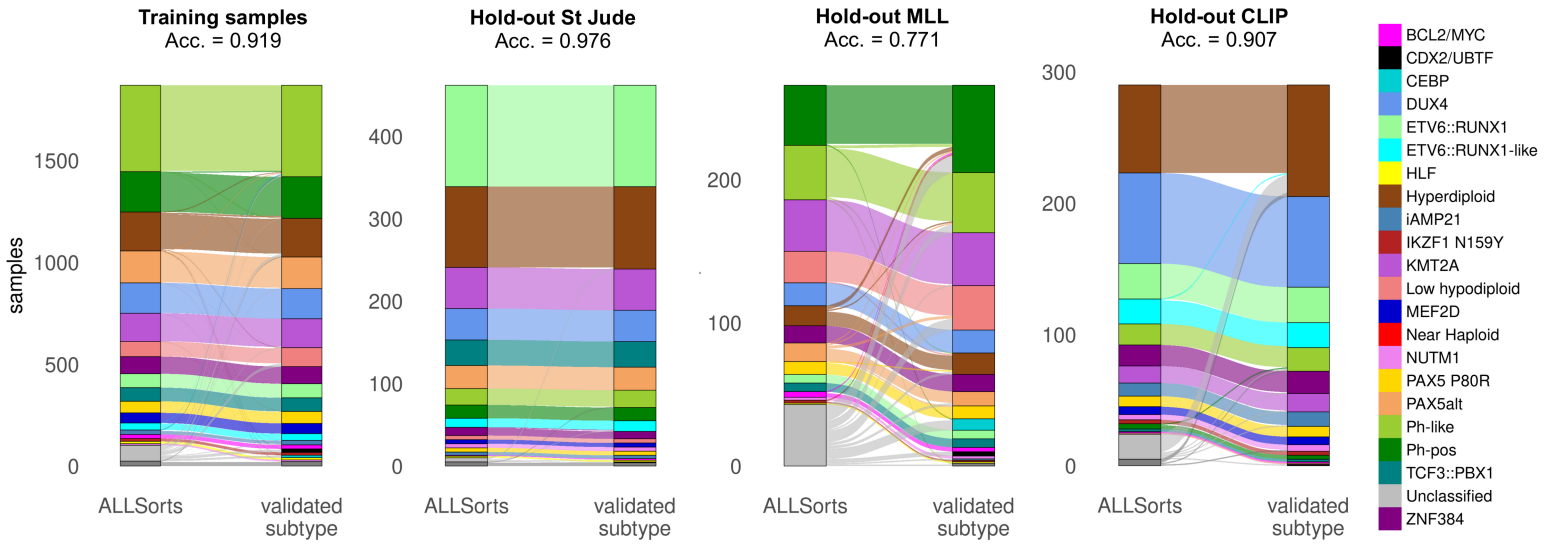

ALLIUM-GEX

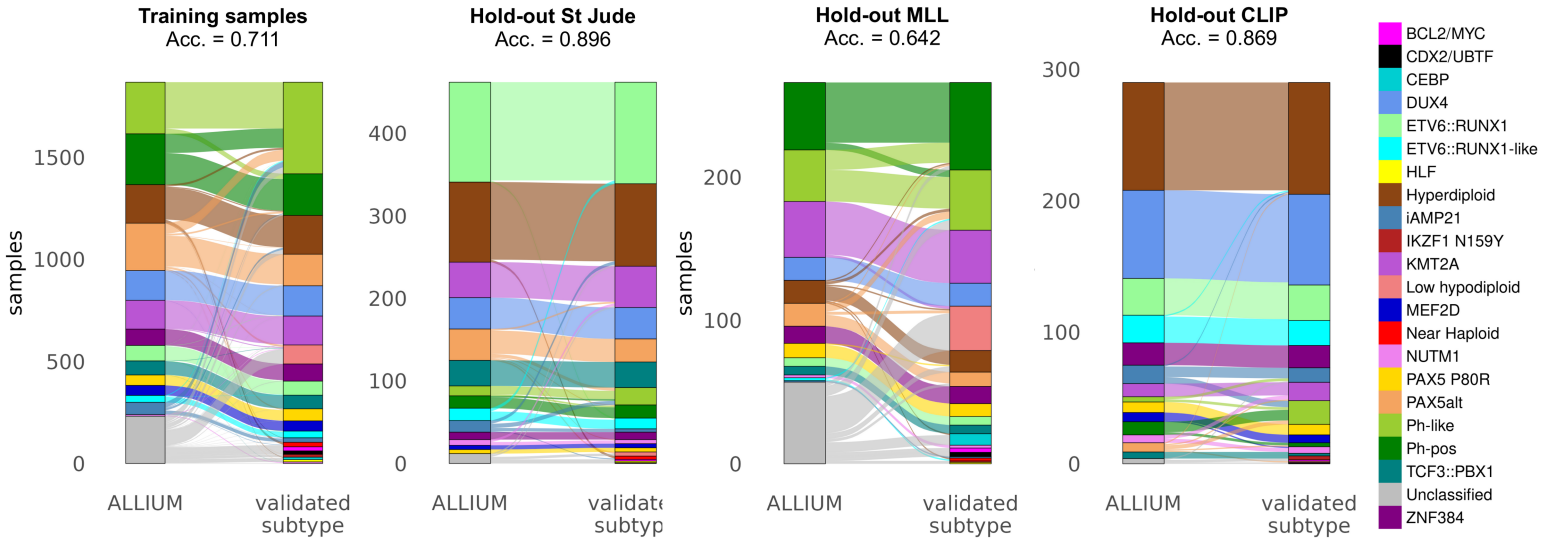

Allspice

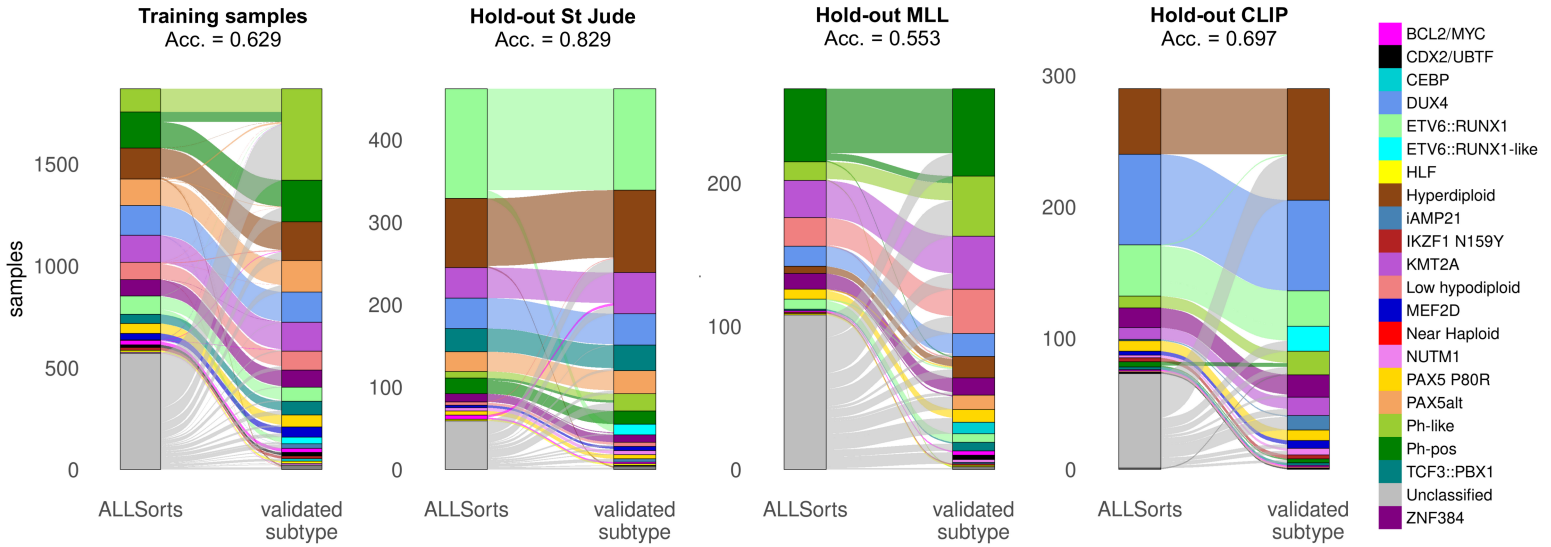

Supplementary Figure S6. Sankey diagrams showing the subtype classification performance of ALLSorts, ALLIUM-GEX and Allspice on the training and hold-out data sets.

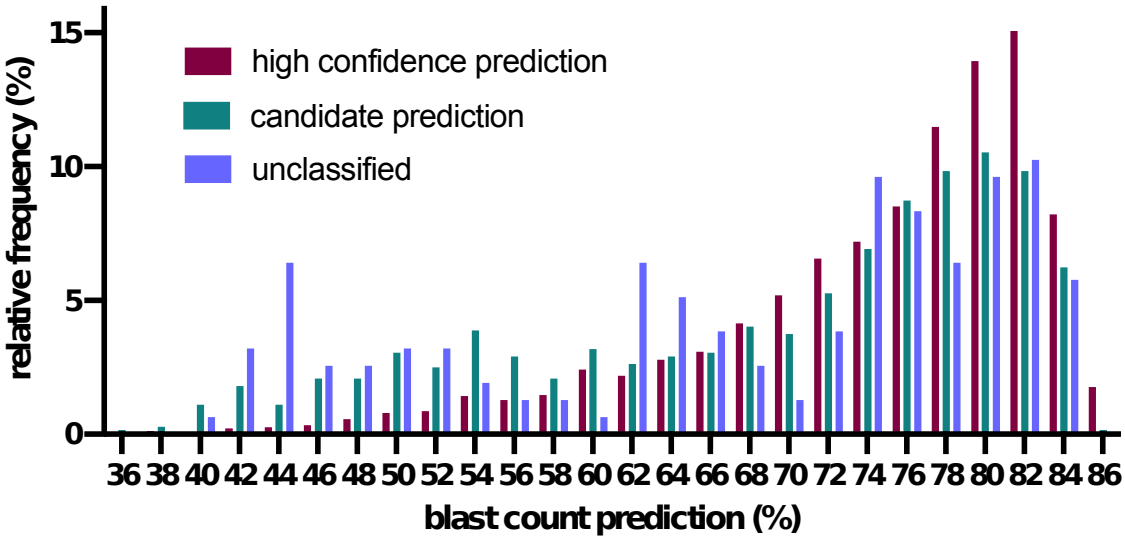

Supplementary Figure S7. Predicted blast counts according to BCP-ALL subtype allocations performed by ALLCatchR. Blast counts were computed for all samples of the combined cohort based on training as described in **Figure 3** of the manuscript. The relative frequency distribution of blast counts is depicted here in relation to the quality of ALLCatchR BCP-ALL subtype allocations. Samples with low blast count estimates are enriched for 'candidate' or 'unclassified' predictions.

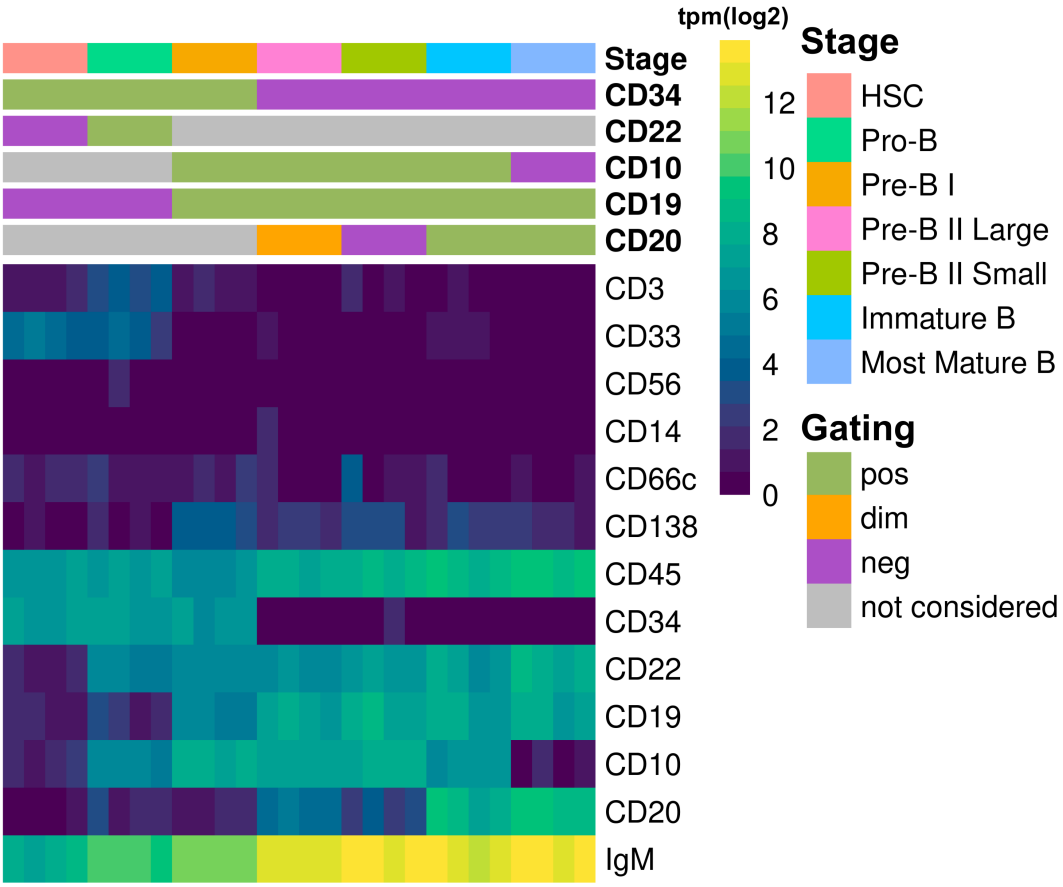

Supplementary Figure S8. Expression of cell surface marker used for FACS sorting of B lymphoid progenitors. Heatmap showing the gene expression values for 13 markers and the corresponding gating schema for the seven B cell progenitors in the annotation rows.

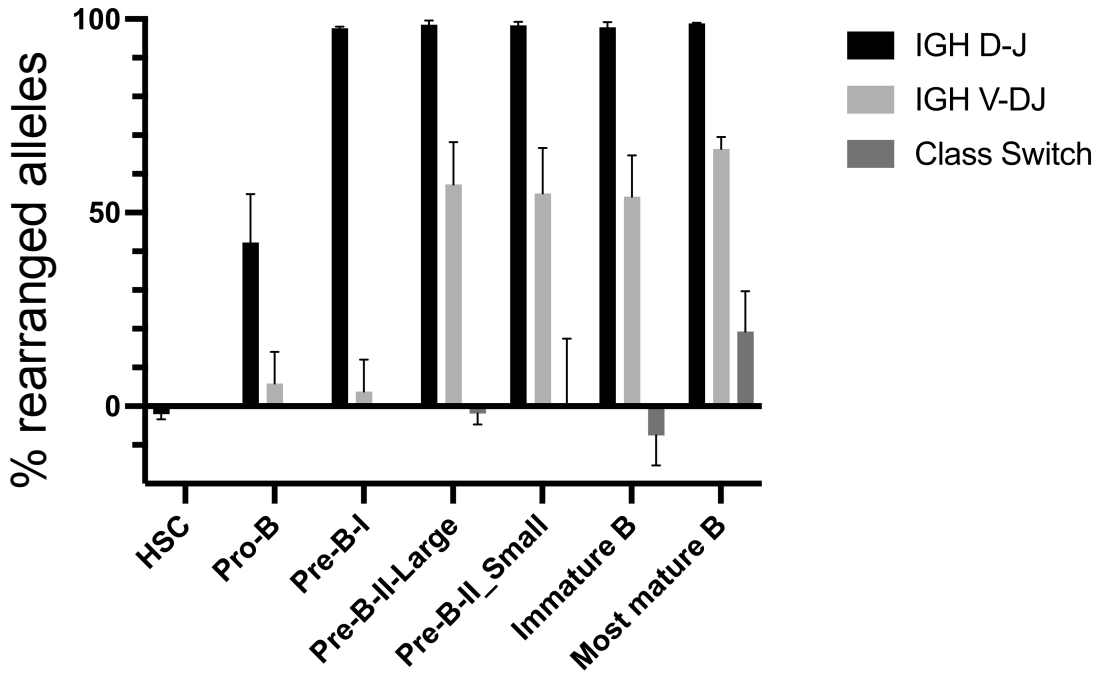

Supplementary Figure S9. Analysis of immunoglobulin rearrangements using droplet PCR. The fraction of rearranged IGH-alleles was measured using a ddPCR that targets the sequences that are deleted during the D-J-, V-DJ- and class switch rearrangements, respectively, together with DNM3 as a reference gene in a multiplex ddPCR setup. The PCR program and the primers and probes were used as previously described. (1) The probes targeting the respective IGH sequences were labeled with a FAM fluorophore and the DNM3 probe with a HEX fluorophore. The 20 µL PCR mixture contained 1X ddPCR Supermix for Probes (no dUTPs) (Bio-Rad), 300 nM of each primer, 100 nM of each probe and 50 ng DNA of interest. Droplet generation and readout was performed as previously specified. (2) The percentage of rearranged alleles was calculated as described. (1)

References to Supplementary Figure S9:

1) Zoutman WH, Nell RJ, Versluis M, et al. A novel digital PCR-based method to quantify (switched) B cells reveals the extent of allelic involvement in different recombination processes in the IGH locus. Mol. Immunol. 2022;145:109–123.

2) Zoutman WH, Nell RJ, van der Velden PA. Usage of Droplet Digital PCR (ddPCR) Assays for T Cell Quantification in Cancer. 2019;1–14

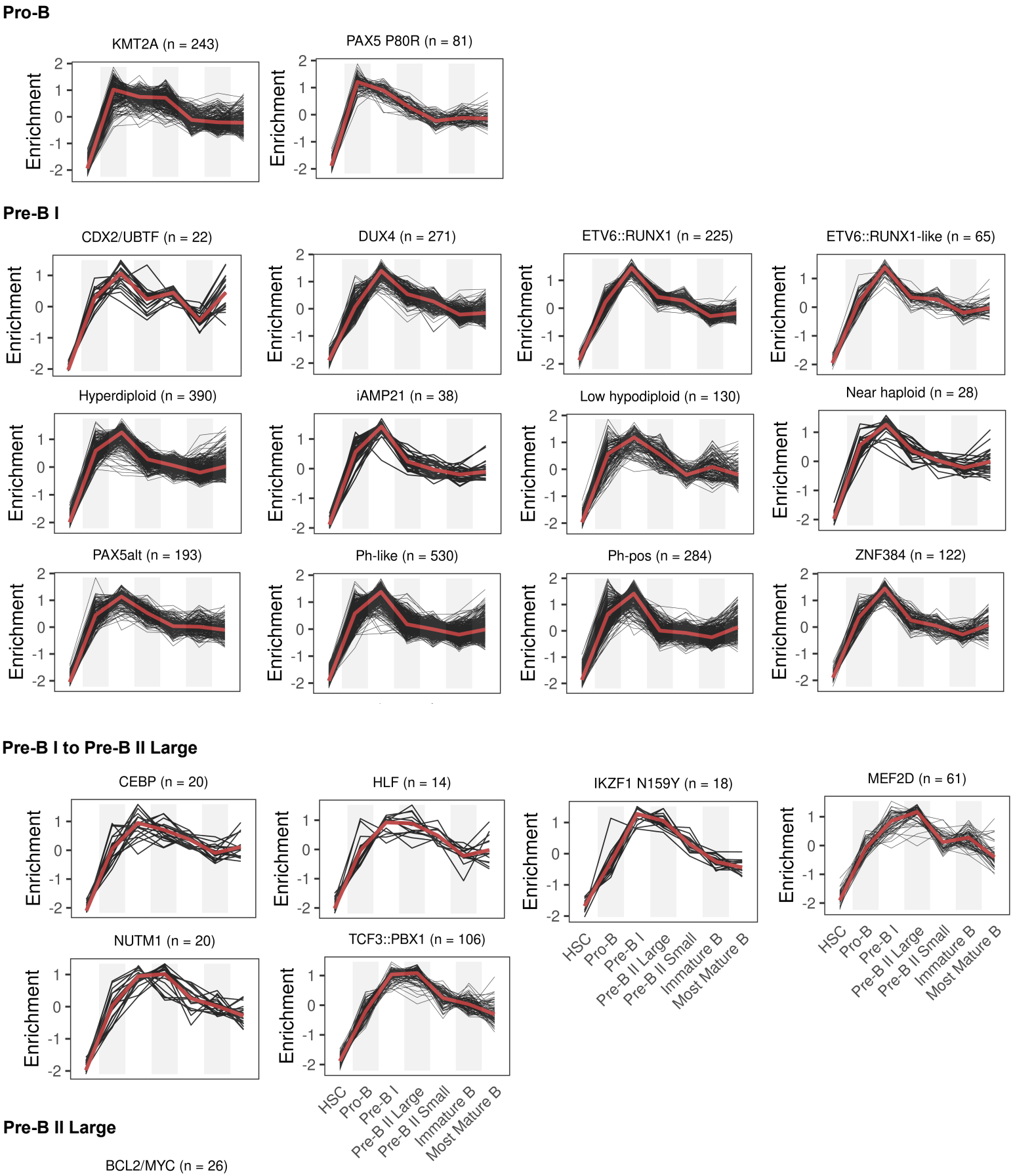

Supplementary Figure S10. Gene set enrichment analysis of BCP-ALL samples shows distinct pattern shared between BCP-ALL subtypes. Single sample gene set enrichment analysis was performed for BCP-ALL samples with defined molecular subtype (n=2,887) and lymphopoiesis-stage specific gene sets (**Figure 4**, main manuscript). Enrichment patterns shared between BCP-ALL subtypes suggest common B lymphopoiesis stages of origin. Condensed heatmap presentations of this data is shown in **Figure 4D** and **Supplementary Figure S11**. KMT2A and PAX5 P80R individual enrichment profiles are shown in **Figure 4E** of the main manuscript and are included here for complete overview.

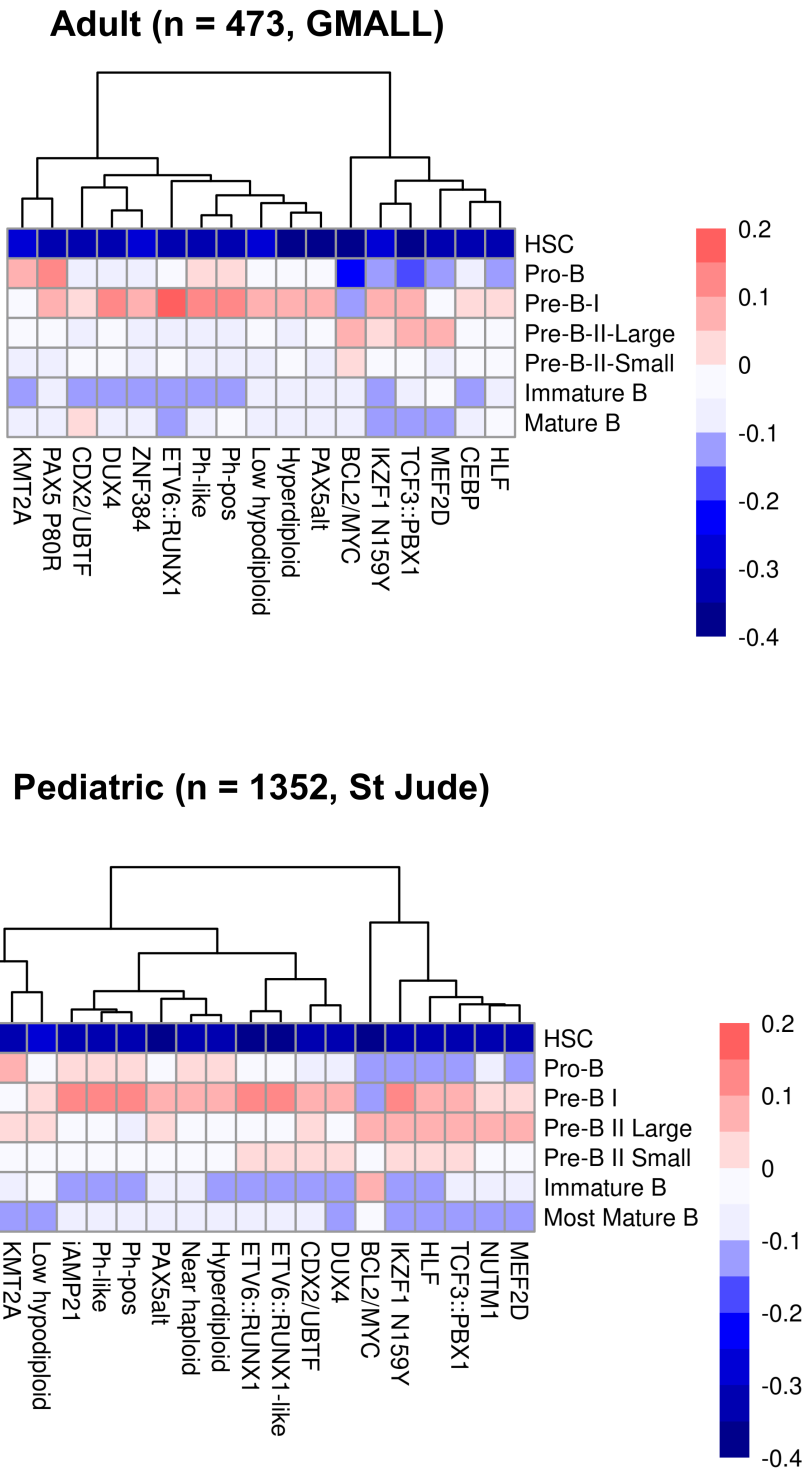

Supplementary Figure S11. Consistent associations to B progenitor gene sets were found in adults and children. Hierarchical clustering of subtypes based on gene expression signatures specific to the seven B lymphopoietic differentiation stages. Adult samples from GMALL and pediatric of St Jude are shown and enrichment scores were averaged for the individual subtypes.

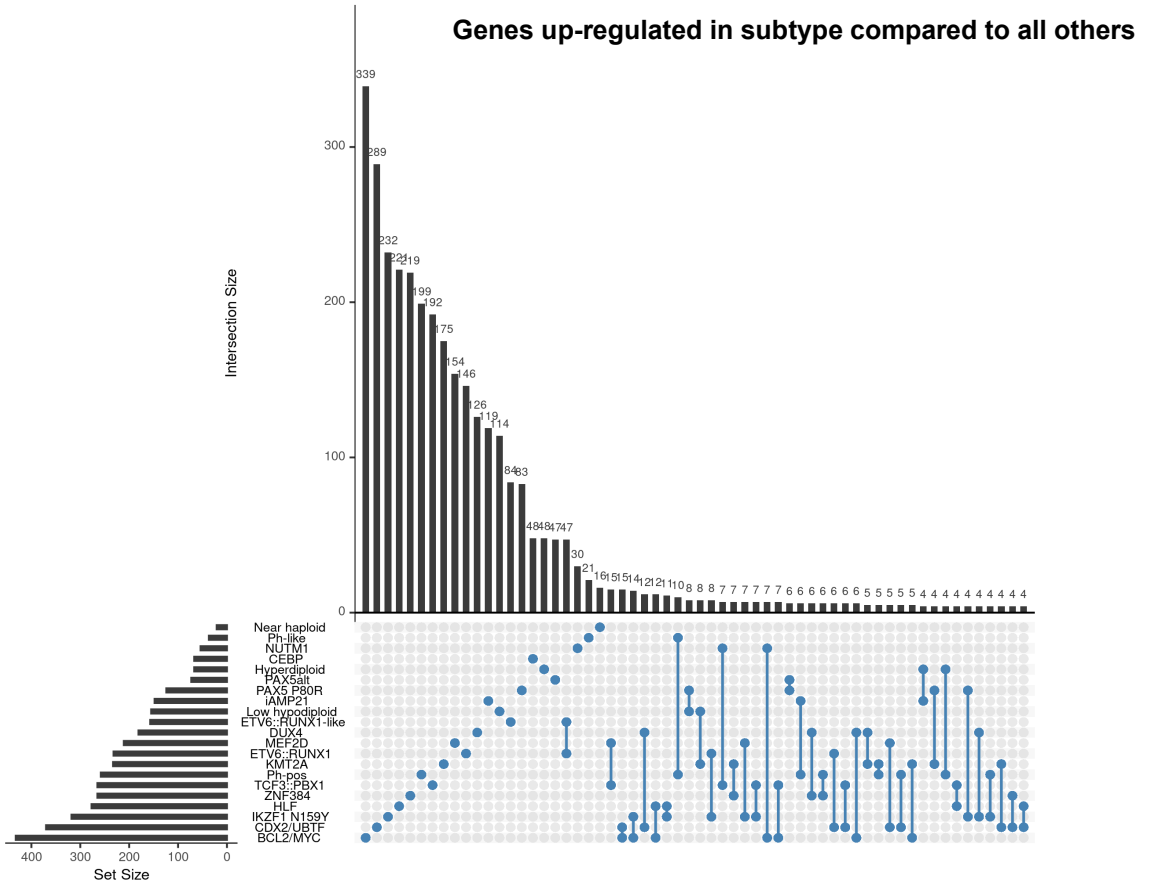

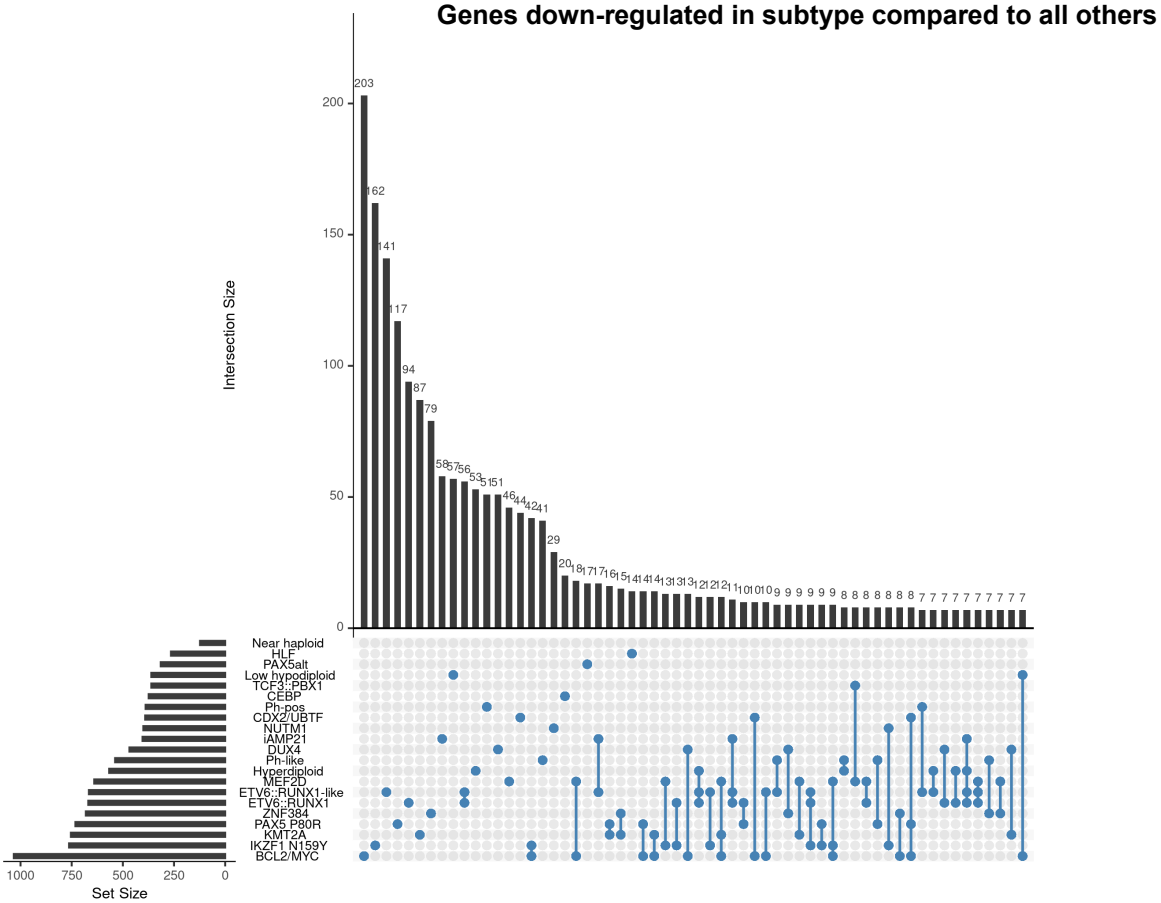

Supplementary Figure S12. Differential expressed genes between BCP-ALL molecular subtypes. Upset plots showing the number of genes (Set Size) for each subtype and the number of unique and shared genes between subtypes (Intersection Size). The plots are truncated for intersections with small number of genes to allow readableness.